Novel Imaging Sensor for High Rate and High Resolution Applications

P. Giubilato and S. Mattiazzo
Dipartimento di Fisica, Universita` di Padova, and INFN Padova, via Marzolo 8, 35131 Padova, Italy.

Square CCD and CMOS arrays are commonly employed to perform two-dimensional imaging tasks as they offer high image quality and spatial resolution. For more specific applications, where the requirement is to locate the position of a fast moving, single luminous spot over a delimited area (single particle positioning, beam spot monitoring, …) such kind of devices is somewhat cumbersome to use, due to the huge number of pixels needed to be read in order to get high resolution the spatial position of the luminous signal. The data throughput limits the use of pixel arrays to those applications where a time resolution of a few hundred frames per second is sufficient. In this contribution we propose a novel device, based on solid state sensors, able to perform two dimensional imaging of a luminous spot with a frame rate (first prototype) of about 10 kHz and a spatial resolution better than 800*800 points over a 25mm diameter circular field of view. A full performance characterization of the first prototype is also reported.

1. INTRODUCTION

1.1. Experimental needs

A novel nuclear microscope (Ion Electron Emission Microscope, IEEM) used for radiation hardness studies of electronic devices has been developed by the SIRAD group at the Legnaro National Laboratory, Padova, Italy [1]. This novel technique, proposed and pioneered for the first time by B. Doyle of SANDIA National Laboratory [2], permits the sensitivity mapping of an electronic device, as it responds to the single impacts of energetic ions, with a lateral resolution equal or better than one micron. This new very promising approach overcomes some of the typical limitations of conventional microbeam systems usually employed for these kinds of applications, but it also poses new challenges concerning the sensing system to employ.

The purpose of these experiments is to correlate the measured response of a complex electronic device exposed to an ion beam with the impact positions of single ions. With enough statistics this correlation results in a map of the ion-sensitive areas of the targeted device. The impact position of the impinging ion is registered by a Photon Electron Emission Microscope (PEEM) which images the Secondary Electrons (SE) emitted by the target surface when the ion strikes on it. A high electric field (up to 15 kV) between the target surface and the transfer lens of the PEEM ensures that the out coming secondary electrons are effectively collected with low lateral spreads. The PEEM microscope focuses the collected electrons emitted from points on the target surface onto a focal plane with a magnification factor typically about 160. By measuring on the focal plane the average position of the cloud of secondary electrons emitted from individual ion impacts it is possible to precisely reconstruct the impact positions on the target surface. Due to the low number of SEs emitted during a strike (some tens, depending on surface type and ion species) and the low PEEM transmission efficiency (roughly 10-30%), only a few secondary electrons actually reach the microscope focal plane. To increase this weak electron signal, a two-stack Microchannel Plate (MCP) is used to multiply the signal by a factor ~10^7. In the SIRAD IEEM setup, the electrons at the output of the MCP hit a phosphor layer (P47) and so generate a light signal that is then collected outside the chamber by means of an optical system. [3]. At the end of the chain, the chosen sensor must be able to acquire the position of luminous spots without degrading resolution and speed.

1.2. Performance requirements

The micron-scale sizes of the smallest active parts of a modern microelectronic circuit (a transistor, a memory capacitor …) requires that to study ion-impact sensitivity of microelectronic devices the nuclear microscope must be able to register the impact position of the impinging particles with a resolution equal or better than one micron. In addition a repetition rate of thousands of ion impacts per second is very desirable to avoid experiments taking too much time.

With regards to spatial resolution, two parameters are of the utmost importance: the area of the target device to be imaged by the PEEM is a circle of 250 μm diameter, and the limiting resolution of the microscope is 0.6 μm (when imaging ion induced secondary electrons). Indeed the required sensing resolution is: 250/0.6 ~ 400 points on the FOV diameter. The amplifying MCP/phosphor stage resolving power is a factor 4 better and hence the resolution of the final sensor is the factor which sets the performance of the sensing chain.

Concerning the time resolution, if one wants to distinguish in time an average of 1000 ion impacts per second, a frame rate ten times higher is required to avoid too many frames with multiple hits.

2. POSSIBLE SENSING SOLUTION

2.1. Analog PSD

The most common solution adopted to perform high speed light spot acquisition is the use of a PSD (position sensitive device). The PSD works on the charge splitting principle: a resistive layer is placed after a depleted junction, which converts the incoming photons to electron-hole pairs. The electrodes at the sides of the resistive layer each gather a charge proportional to the spatial position of the total charge generated. The main advantages of this type of device are the relative simplicity of use and the good event rate it can handle. Like all other charge splitting systems, resolution depends on the ratio between the collected charge and the proper noise. A suitable sensor for the IEEM microscope has been designed around this kind of sensor, but the measured performances never matched the expected result due to the high electromagnetic noise picked up by the large sensor employed (2cm × 2cm).

2.2. Pixel Array

Another possibility is to use a CCD or CMOS pixel array as a position sensitive detector. Both CCD and CMOS technologies offer systems with resolutions up to mega-pixel level, so our minimal requirement of 400 points on the image diameter is certainly not an issue. The main advantage of these devices is that the position information does not depend on the signal level: every signal above the noise level and inside the dynamic range will give position information with a resolution only very slightly dependent on the signal strength.

The drawback of this approach is the need to read the entire pixels array to determine if and where the light-spot arrived. Assuming a small square CCD of 256 by 256 pixels, already sufficient to reach a resolution of 400 points with basic data fitting (weighted averaging on hit pixels), the number of pixels to be read for each frame is 65,536. Considering that a minimum 8 bit depth per pixel is required to have a good dynamic range, i.e. to have the capability of handling signals with different intensity levels, the total data stream per frame will be equal to 65kByte/frame.

The data throughput for a 10 kframe/s acquisition results of the order of 0.6 Gbyte/s. This number highlights the first great difficulty in following this approach: 0.6 Gbyte/s is a quite difficult data stream to maintain for an entire session run (seconds, minutes, hours…). But, even with a system able to sustain the requested data throughput, a second problem arises: data coming from the sensor must be processed in order to find, within every frame, where the ion impact occurred, if any at all. To perform real-time analysis on such a huge amount of data is a task that completely overcomes the possibilities of any small to medium experimental apparatus. Moreover the main drawback of CCDs (or CMOS) classic approach is the huge number of pixels to read for each frame. Assuming to have one registered light spot from a single ion impact event per frame, this means that 99.97% of data readout capabilities are exhausted for reading empty pixels that carry no useful information.

The numbers stated above are just sufficient for the minimal IEEM detection requirements. A more performing system minimally suited to IEEM spatial resolutions, e.g. a 512×512 pixels sensor, giving an equivalent resolution better than 1000 linear points and running at frame rates of the orders of 100 kframe/s, would raise the complexity of the problem by about three orders of magnitude. Therefore, outperforming the PSD detection capabilities with straightforward CCD arrays appears to be nearly impossible.

A third way could be the use of CMOS technology to perform on-chip data reduction, as recently offered by first commercial available solution [4]. CMOS technology allows packing some electronic components (amplifier, discriminator, etc.) with each pixel, allowing a greater flexibility than CCD, where signal is sequentially extracted from every charge well. Although this is probably the best solution to the problem of high-speed, high-resolution single light spot detection, the lack of a commercial demand for such a kind of device makes them at present available only as custom made, single model, R&D experimental devices.

3. A NOVEL SYSTEM

3.1. Concept

From what was discussed above, it seems that the only present commercial available device able to satisfy the given requirements is the analog PSD. However, its use has also been shown to be somewhat unreliable and not entirely satisfactory.

A different solution was pursued by developing a CCDs based system. As already mentioned the use of CCDs, or conceptually similar devices, is attractive because the working principle ensures resolution performances uncorrelated to the signal strength. A digital system, moreover, would allow a greater flexibility in data manipulation respect to the analog PSD one. Dramatically reducing the number of pixels to read would make the use of CCDs a more feasible solution. To reduce the number of pixels, one efficient way is to consider the orthogonal projections of the detected light event, as sketched in Figure 1. Working on the projections only, the number of pixels to read is reduced to the square root of the size of the array (with a parallel reading of the two projections), while the spatial resolution remains unaffected.

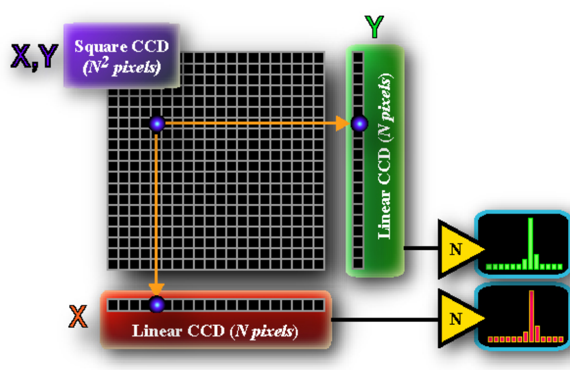

Figure 1 – Using two linear arrays to read only the projections of the spot dramatically reduces the number of pixel to read, from N^2 to N.

Furthermore, data analysis becomes easier due to the simplicity of the resulting output signal: a peak on the projection will indicate the position (in that coordinate) of the registered light spot. Minimal peak fitting procedures makes possible enhancing the bare sensor resolution by at least a factor two. The main drawback of this solution is the difficulty to distinguish more than one ion impact per frame. If two (or more) events have different projected coordinates, the position of each event can be reconstructed watching at the height of the registered peaks and then matching peaks of equal eight. In the case of superimposed coordinates or of identical strength signal, reconstruction becomes impossible. Anyway, working with a maximum of a few events per frame (n), the possibility of dealing with superimposed coordinates is quite low (proportional to 2n/array size). While in the analog PSD the original information, i.e. the real position of incoming light spots, is completely lost in case of multiple events, this does not happen with the projection solution. Even if a multiple event (per frame) reconstruction would not be possible due to ambiguity in assigning coordinates, the available information could still prove to be useful.

Let us consider the simple case where every event generates a cluster of signals, and one or two signals, widely separated from the cluster (Figure 2). The isolated signals would affect the reading of an analog system that returns the weighted mean position of the total charge collected. Instead the isolated signals are easily recognized by the digital system, allowing one to decide whether or not to account for them for the position calculation of the ion impact in this frame.

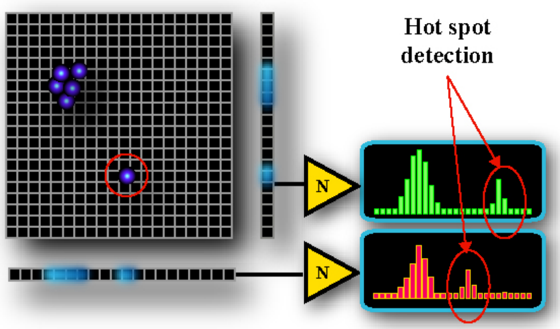

Figure 2 – Hot spots or spurious signals can be recognized and consequently not used in position calculation, an impossible task for any analog PSD system.

3.2. Realization

To make a system work according to the projection method the first step is to get the two projected images of the light signal, as illustrated in Figure 1. The straightforward solution to this task is the use of CMOS technology with device-level electronics dedicated to sum per rows and columns the signal of each photodetector, thus allowing projection capabilities. The output of a similar device would be identical with that discussed for CCDs in previous paragraph. However, the few available commercial devices with this characteristic offer low speed and low resolution with a small photodetectors size (the area of each pixel), which means a very poor behavior with low light signals.

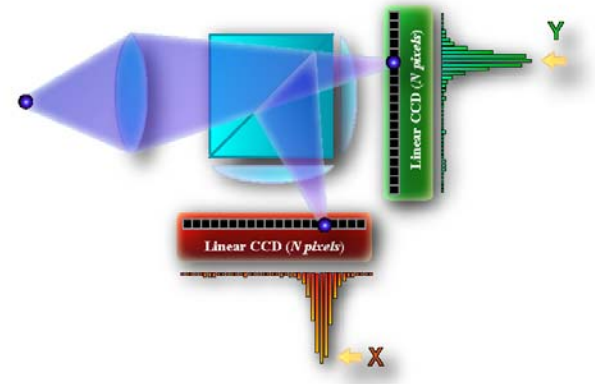

Figure 3 – Optical projection system is a fast and reliable way to decrease the number of pixels to read by flattering the original image from 2D to 2×1D.

Nevertheless, the same result can be achieved working on the light signal itself before it reaches the sensing array. A novel electro-optical device developed around this idea was first proposed [5] and realized by us in order to give superior position detection performances (Figure 3). An optical system splits the original image into two copies, and then squeezes each copy into one-dimension. This means that a single bright point of x, y coordinates in 2D space is rendered as two separate points, one representing the x coordinate, the other representing the y coordinate. The projected and squeezed images are then acquired using conventional linear CCD. The use of optics presents advantages and disadvantages. It is fast, reliable and accurate, but also introduces geometrical distortions and, when a precise measure of the signal light intensity is a concern, non negligible vignetting effects. We will show in the next paragraph how these problems were solved in this first working prototype.

It is useful to carry out some simple estimations about the potential of this approach. First, it relies only on commercial and well-established technology (CCDs, optics). Second, while the optical part of the arrangement is quite stable, the reading components, that ultimately define the system resolution and speed, can be easily upgraded to follow the development of state of the art devices. Most modern imaging devices offers data throughput up to 40÷50 MHz per channel. For a 512 pixels linear array this means a maximum frame rate of 78 kframe/s. This value can be raised by lowering the resolution or by using a multi channel device for parallel data output. It must be noted that to match the present analog PSD resolution performance a 256 pixels sensor array is far enough. Numbers above reported refer to a hypothetical device with an equivalent resolution of more than 1200 linear points and a resulting data output of 40 Mbyte/s for 8 bit depth pixels, to compare with the 25 Gbyte/s for a conventional square array with the same resolution.

Many high-grade CCD devices offer a random noise lower than 50 e^-/pixel, allowing for extremely low light signal detection impossible with conventional PSD systems. Furthermore, the great flexibility of this approach allows optimizing the tradeoff between resolution and speed quite easily.

3.3. Optics

The optical system is the core of this novel PSD apparatus. It splits the incoming image and focuses the projections onto the linear sensors. To perform this task cylindrical lenses, i.e. lenses that act in only one axis, are orthogonally placed along the two optical paths resulting from the image splitting. In Figure 4 the arrangement of the lenses system is sketched. On the left (incoming image side) a light spot is moving along the Y-axis of the object space, does not matter what is happening along the other axis. Now, due to the presence in the optical path of non-symmetrical elements (the highlighted cylindrical lens), the imaging behavior is different between the X and Y axes of the optical path.

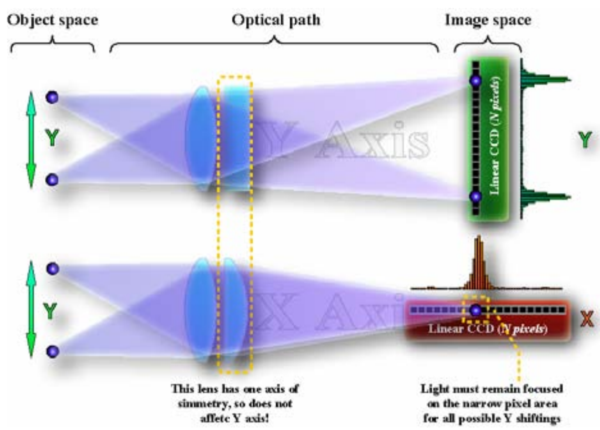

Figure 4 – STRIDE optical scheme exemplification, illustrating a light spot moving along Y axis into image space. The optical path does not present a classical cylindrical symmetry, so while the highlighted lens acts along the X-axis of the optical path by squeezing the image, it does not affect the Y-axis, that works like a classical optical relay scheme.

These axes coincide with the object space X and Y axes. Along the Y-axis of the optical path, the only active elements is a conventional relay lens (the first lens on left), as the other lens does nothing in this orientation, which simply focuses an image of the moving spot into the linear array. On the contrary, into the X-axis the cylindrical lens acts squeezing the image along this axis, providing a light spot on the X-axis array that is not sensitive to movement of the source along the Y-axis. This arrangement allows using two linear sensors instead of a square one, as each sensor see only the projection along one axis of the incoming light.

3.4. Electronics

The sensor employed into the first prototype is a Hamamatsu S3901-256 NMOS linear array [6]. It was chosen for its ease of use and its huge pixel height (2.5 mm), a characteristic that well matches the light blade output of the optical system. The main drawback of this family of sensors is their very low speed: only 2 MHz readout. With this readout speed the resulting frame rate is $2\times10^6/256 \sim 7800$ frame/s; over clocking to 4 MHz would obviously double the speed. In our prototype a 3.125 MHz clock is applied, thus the frame rate is equal to 12.2 kframe/s.

Proprietary electronics was developed to both drive and read the two linear sensors. In order to get a flexible system capable to work with different types of devices (CCDs, NMOS, …) every output clock line (up to ten) has its own tunable swing range and separate output buffer. Two fast (40 MHz) 12 bits ADCs (one per axis) convert the analog signal read from the sensor into digital format. An USB port provides the connectivity to the control PC. The entire system is controlled via a Xilinx VirtexII FPGA loaded with proprietary firmware. The FPGA provides the clocks for all the components, handles the communication protocols for the USB port and processes the data incoming from the two ADCs.

Even though greatly reduced respect to an equivalent square sensor, the data throughput from the two linear sensors is still quite heavy. Even at low speed (10 MHz), it means at least 20 MB/s of continuous data to analyze. This data rate would fill the band-width of most common PC interfaces, GBit Ethernet included, when considering a sustained continuous data rate. Moreover, always referring to consumer available technology, real-time analysis of such a quantity of data becomes also a concern, even with the fastest available computers and optimized codes. To overcome these bottlenecks, all the analysis has been implemented into the FPGA device that controls the entire system. Digitized data incoming from the ADCs are parallel processed and the position of (the possible) light spot is detected and fitted. When an event has been identified, it is sent to the control computer as a data packet of 8 bytes. This sets, independently from the frame rate of the sensors, the maximum sustainable event rate. Assuming to have a transmission band width of 1 Mbyte/s, the maximum average event rate will be 62,000 events/s. This value refers to the average rate only, as buffering can be employed to sustain bursts of higher frequency. Widely available commercial standards exist, for example USB 2.0 which gives data throughput greater than 10 Mbyte/s, so that the hardware analysis ensures enough power to handle event rates near the million events per second limit. The limit on the event rate actually comes from the speed of the sensor, while the data analysis is an addressed issue.

4. RESULTS

4.1. Resolution

To measure the random error on position recognition the field of view (25 × 25 mm^2) was scanned with a LED-illuminated spot on a matrix of 30 by 30 steps. At every position 10^4 measures were taken and the dispersion calculated. Reported values give the position reading uncertainty expressed in 1/1000s of the FOV diameter (25 mm). This representation makes easy to match these values with those reported in next paragraph about distortion (systematic error). The equivalent linear resolution expressed in resolvable points on image diameter is simply equal to 1000 divided by the reported value. White area in Figure 5 set the limit of acceptable resolution, as 1000/2.5 = 400 points. Inside near all the actual watched area, that is circular, resolution performance is everywhere better than 650 linear points, and within the 70% central region is superior to 1000 linear points. The noisy corner on the bottom-right of the graph is due to a little misalignment of the optical axis, which results in a non symmetrical light collection on areas at the borders.

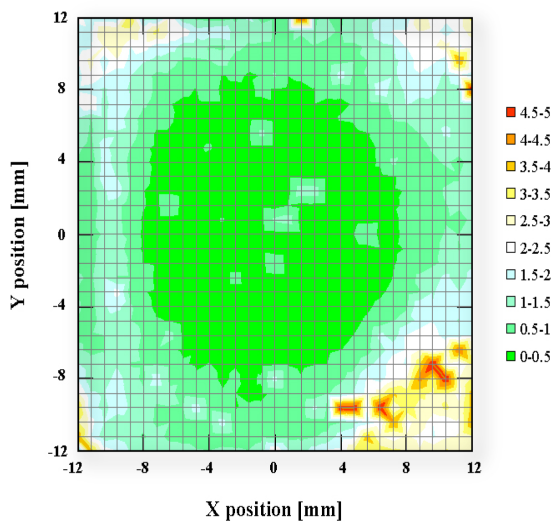

Figure 5 – Spatial resolution over the entire FOV. Values express resolution in point per thousand of the FOV diameter (25 mm).

4.2. Distortion

Distortion is a systematic error, so in principle it is possible to deal with it. Nevertheless, as the precision with which we take measurement is finite (limited by resolution), distortion actually leads to wasting a certain amount of information. This can be easily exemplified considering when, because of the optical distortion, two different points are focused on the sensor at a distance smaller than its spatial resolution (image plane). Due to resolution limit, it will be no more possible to distinguish them, even if their original distance (object plane) was proven to be resolvable. Collection efficiency was partially sacrificed in order to have an optical system with intrinsic low geometrical distortion. Figure 6 shows the distortion measured in the same test conditions reported in previous paragraphs.

Distortion has been evaluated by measuring the distance between the original light spot position (known with a precision better that 1 μm thanks to the sub-micron resolution of the XY micro-positioning stage) and the acquired position. The average of all readings taken to evaluate the random error has been used as true value of the measured position, thus making non-systematic errors negligible.

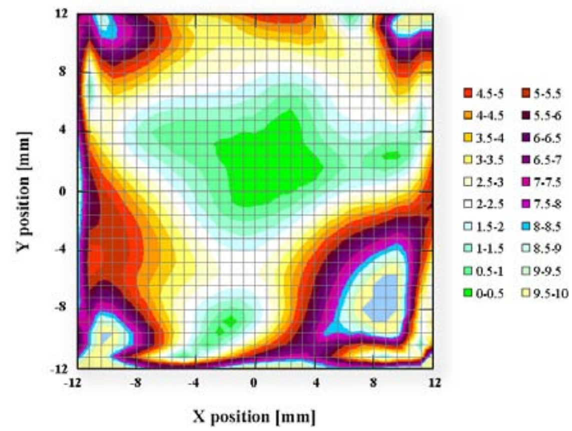

Figure 6 – Geometric distortion over the entire Field of view. Values express distortion in points per thousand.

As the scale used to plot the graph is the same as in Figure 6, it is easily to note how the systematic error is bigger than the random one. Outside the very central region around the optic axis, where the magnitude of two error sources is similar, distortion error results to be at least two times bigger than random noise. However, the measured distortion represents a quite remarkable result, being under 0.5% for the very majority of imaged area and under 1% in the entire field of view. Such a good distortion performance is usually a prerogative of metrology optics used in gauging applications.

The little misalignment between the optical axis and the two sensor planes are here more evident than in the random error plot: for a perfectly tuned system, geometrical distortion should appear symmetric respect to the X and Y axis. This error has been fixed thanks to a new mechanical housing, which was still under construction during these tests. By enabling the software correction system, distortion can be real-time corrected.

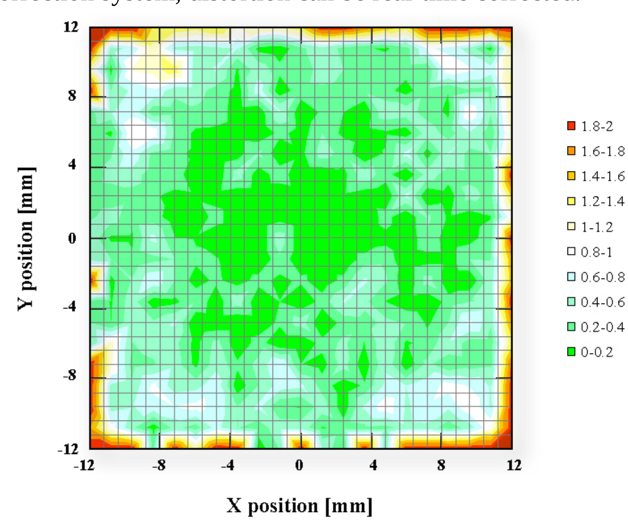

Figure 7 – Distortion measured with software correction enabled. Values expressed in points per thousands. Color scale is different respect to Figure 5 and Figure 6.

The same test procedure was repeated, with the software correction enabled, only changing the matrix steps in order to avoid any position superimposition, a too easy condition for the correction algorithm. Data plotted in Figure 7 are not the result of post processing operations, but the original data recorded by the control software, exactly as in Figure 6. Systematic errors are smaller than 0.5 ‰ over the entire field of view, in fact smaller than the random error even at the border of the image. Only on the corners, the rectification algorithm fails to cancel the systematic errors. Systematic errors smaller than the random errors allows one to consider this device a distortion-free system.

4.3. Vignetting

Vignetting is the term used to describe the loss of brightness that occurs at the image corners due to the non-uniform light transmission of the optical system. In a more general sense, we can speak of vignetting regarding all the light transmission efficiency variation caused by the optical system when moving across the field of view.

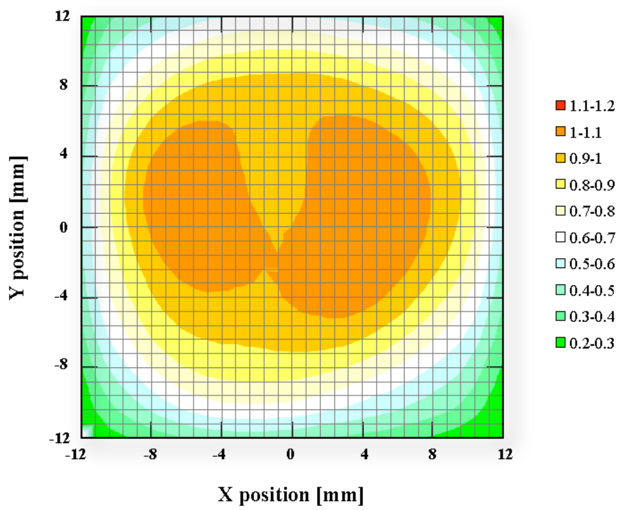

Figure 8 – Vignetting maps over the FOV. Values represent brightness ratio respect to the one measured on the optical axis (X = 0, Y = 0).

Usual optical systems show maximum transmission efficiency for on-axis points and a gradual decrease near the FOV borders.

Our optical system is a bit more complex, and consequently exhibits a nonlinear vignetting pattern, as illustrated in Figure 8. In this graph, the colour scale indicates the ratio between the brightness value measured at the indicated point and the brightness value measured on the optical axis (X = 0, Y = 0), used as reference.

Over the useful image area the brightness ratio ranges between 0.5 and 1. Even if this represents a quite good result for such a kind of optical system, it is not satisfactory at all for performing scientific measurements.

As in the case of geometrical distortion, the ability of the correction algorithm in handling vignetting has been carefully evaluated by repeating the measurements with a different grid step after enabling the correction routine. Results are plotted in Figure 9. After correction, the registered signal level shows a variation smaller than 2% over the entire FOV, a performance that allows a much more accurate evaluation of the original light signal intensity. The extremely low vignetting level obtained allows using the event luminosity (proportional to the registered peak height) as recognition parameter in case of multiple events per frame.

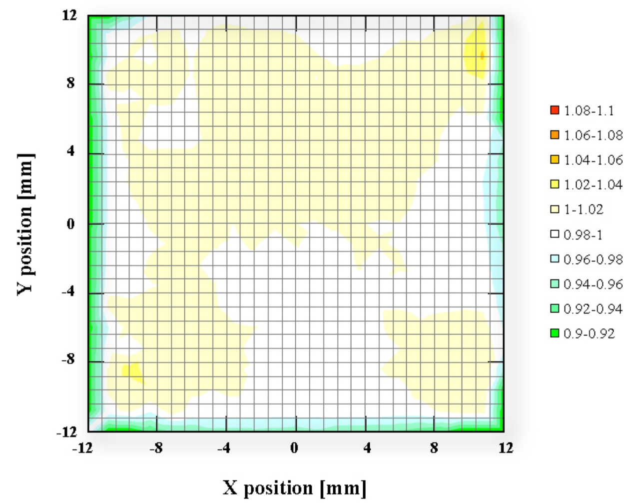

Figure 9 – Vignetting map with correction enabled.

5. REFERENCES

[1] D. Bisello, M. Nigro, J. Wyss, A. Magalini, D. Pantano, A. Kaminsky, S. Sedyck, “Ion Electron Emission Microscopy at the SIRAD single event effect faciliy”, Nucl. Instr. And Meth. B, vol. 181, pp. 254−257, 2001.

[2] B.L. Doyle, G. Vizkelethy, D. S. Walsh, B. Senftinger and M. Mellon., Nucl. Instr. Meth. B 158 (1999) 6.

[3] BURLE instruments QS 11983−2: APD 3040PS 12/10/8 I 60:1 6.4CH P47 two stack, 40 mm diameter with 8 mm central hole diameter MCP coupled to a P47 phosphor layer.

[4] Hamamatsu S9132 CMOS Profile sensor.

[5] D. Bisello, M. Dal Maschio, P. Giubilato, A. Kaminsky, M. Nigro, D. Pantano, R. Rando, M. Tessaro and J. Wyss, “A novel sensor for ion electron emission microscopy”, Nucl. Inst. and Meth. B, vol. 219−220, pp. 1000−1004, 2004.

[6] Hamamatsu S3901/S3904 NMOS linear image sensor.